SCIENCE CHINA
Chemistry

•FEATURE ARTICLES•
SPECIAL ISSUE: 2021 Emerging Investigator Issue

November 2021 Vol.64 No.11: 1923–1937
https://doi.org/10.1007/s11426-021-1068-2

Bimetallic anchoring catalysis for C–H and C–C activation

Jiang-Fei Li, Yu-Xin Luan* & Mengchun Ye*

State Key Laboratory and Institute of Elemento-Organic Chemistry, College of Chemistry, Frontiers Science Center for New Organic Matter, Nankai University, Tianjin 300071, China.

Received June 3, 2021; accepted July 11, 2021; published online September 17, 2021

Following the age of directing group, anchoring catalysis starts coming to the center of the stage. Different from the directing-group strategy that needs a preinstalled directing group in substrates, anchoring catalysis relies on a reversible interaction between a substrate and a catalyst, which then directs metal to activate inert chemical bonds. Such reversible directing effect not only generates good site- and stereo-selectivity as traditional directing groups do but also eliminates the requirement of stoichiometric amounts of directing groups. Among variously reported anchoring catalysis, coordinative bimetallic anchoring catalysis in general displays superior reactivity than others because coordinative bonding not only affords strong interaction of catalysts with substrates but also displays good compatibility with substrates and reaction conditions. In recent years, big progress has been achieved for coordinative bimetallic anchoring catalysis. This review gave a detailed summary of this field, including catalyst development, catalyst types, reaction types and reaction mechanisms.

C–H activation, C–C activation, bimetallic catalysis, enantioselective, anchoring catalysis

Citation: Li JF, Luan YX, Ye M. Bimetallic anchoring catalysis for C–H and C–C activation. *Sci China Chem*, 2021, 64: 1923–1937, https://doi.org/10.1007/s11426-021-1068-2

1 Introduction

Due to the ubiquity of C–H and C–C bonds in organic molecules, the development of robust methods for their direct transformation is of importance for organic synthesis [1], because such a transformation not only eliminates the need for pre-functionalization of starting materials, thus providing an atom- and step-economical route to organic molecules, but also allows the use of readily available chemical resources, thus significantly expanding the source of substrates. However, compared with activation of other bonds such as C–X (Cl, Br, I), C–O and C–N bonds, C–H or C–C bond activation is faced with a tremendous challenge because of their higher bond energy and overwhelming prevalence with often-marginal chemical differences in organic molecules. Various catalytic methods have been explored during the past several decades to address this challenge, and finally, transition metal catalysis stands out among them [2], because transition metal catalysts, together with proper catalytic strategies, present more versatile reactivity and higher catalytic efficiency in most cases.

The early-stage catalytic strategy for C–H activation is to incorporate an active reagent into substrates to facilitate the interaction of substrates with metal catalysts, thus ultimately promoting reactivity and selectivity [3]. However, this intramolecular reaction design suffers from significant limitations, including tedious substrate preparation and limited product diversity. Directing group strategy emerges and rapidly occupies a central position in C–H or C–C bond activation reactions to address these limitations [4]. In this strategy, a proper directing group is preinstalled into substrates to coordinate a metal catalyst, thus facilitating inert bond activation and product-complexity construction. Directing group strategy proves successful, and considerable progress has been achieved for C–H and C–C bond activations during the past two decades. Nevertheless, significant

*Corresponding authors (email: mcye@nankai.edu.cn; yxluan@nankai.edu.cn)

limitations still exist. First, additional synthetic steps are often required for the installation or removal of customized directing groups. Second, the use of stoichiometric amounts of directing groups would result in a low atom economy, especially when a directing group is comparable to a substrate. Third, it is difficult to install directing groups into raw materials such as simple arenes and alkanes. In this context, the development of new strategies to facilitate C–H or C–C bond activation without special directing groups is highly desirable.

Inspired by enzymatic catalysis that anchors a metal catalyst and a substrate in a protein pocket to undergo highly efficient catalysis, chemists devise synergistic catalysis to address this challenge, and soon a large number of relevant concepts emerge [5], including catalytic amount directing group, transient directing group, bimetallic catalysis, cluster catalyst, supramolecular catalysis, scaffolding catalysis, tandem catalysis, cooperative catalysis. Despite different names, most of these strategies share two critical features as those in enzymatic catalysis: (1) a bifunctional catalyst that can bind a substrate first and then selectively activate a certain C–H or C–C bond of the substrate; (2) the interaction between the substrate and the catalyst is reversible, thus allowing an easy regeneration of the catalyst after the reaction. To unify these strategies and highlight their common characters, herein, we coin "anchoring catalysis" to describe these catalytic processes and a general depiction is shown as below (Scheme 1).

In principle, reversible interaction between substrates and catalysts includes reversible covalent bonding, H-bonding, coordinative bonding, ion-pair bonding, π-stacking, and even dipole-dipole interaction, like those found in enzymatic catalysis. However, owing to relatively harsh conditions required for C–H or C–C bond activation, up to now, only four relatively strong interactions such as reversible covalent bonding, H-bonding, coordinative bonding, and ion-pair bonding have been successfully applied to C–H bond activations, whereas weak interactions such as π-stacking and dipole-dipole interaction still cannot provide good directing effect in such reactions [6].

Among four strong interactions, reversible covalent bonding through reversible C=N bond or O–P bond has been extensively explored in C–H bond activation reactions, and relevant progress has been summarized in several reported reviews [7]. In contrast, the development of the other three non-covalent bondings, including H-bonding [8], coordinative bonding, ion-pair bonding [9,10] in C–H bond activation reactions, is still in infancy, in spite of their more promising features such as rapid dissociation of catalysts from substrates, and good functional-group compatibility. Among these three non-covalent bondings, coordinative bonding is relatively more superior because it possesses stronger coordination with substrates and wider substrate scope. Therefore, coordinative bonding catalysis has received more intensive attention in recent years. To form a proper coordinative bonding between a substrate and a catalyst without inhibiting the following C–H or C–C activation, an extra metal (M_2) beyond metal catalyst (M_1) should be introduced into the catalyst (Scheme 2). In addition, in order to obtain the desired directing effect as that in the directing-group strategy, a proper linker between two metals should be used to generate good synergism of two metals.

In general, there are three types of linkages for these two metals: metal ligation, metal anion ligation, and ligand ligation. According to linkage types, bimetallic anchoring catalysis (BAC) through coordinative bonding can be divided into three groups: (1) metal-ligated BAC; (2) anion-ligated BAC; (3) ligand-ligated BAC (Scheme 3). One of two metals in BAC is a real catalyst, and the other provides anchoring interaction with a substrate, thus generating a directing effect before the step of C–H or C–C bond activation. Notably, the current bimetallic catalysis is quite different from traditional bimetallic catalysis, wherein two metals act as both catalysts [11] and both anchoring sites without synergistic directing effect [12].

Recently, big progress has been achieved for coordinative-bonding anchoring catalysis, and many examples with good yield and selectivity and even high enantioselectivity have been reported for both C–H and C–C bond activation, opening a new avenue towards the activation of various inert bonds. Although many examples still cannot give solid

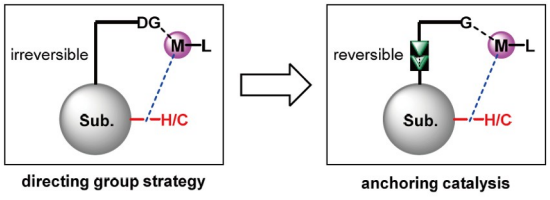

Scheme 1 Anchoring catalysis (color online).

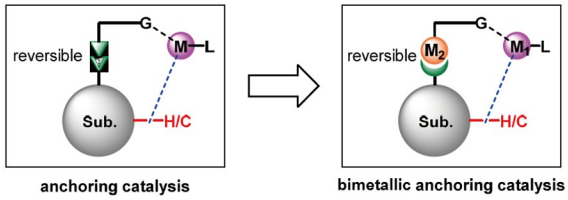

Scheme 2 Bimetallic anchoring catalysis (color online).

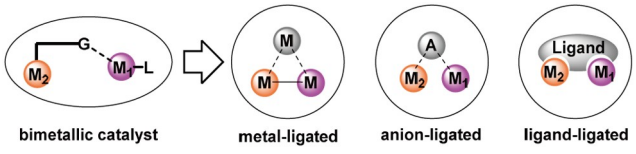

Scheme 3 Types of bimetallic anchoring catalysis (BAC) (color online).

evidence on bimetallic anchoring catalysis, relevant reactivity and selectivity can be well explained by this catalytic mode. Herein, we will highlight advances in this topic and give a summary on catalyst development, catalyst types, reaction types and reaction mechanisms.

2 Metal-ligated BAC

Metal-ligated BAC means that a third metal is used to ligate the other two metals that act as a substrate-anchoring site and a catalyst to activate C–H bonds. Such a catalyst appears in general as a tri-nuclear metal cluster.

In 1982, Shapley and co-workers [13] used stoichiometric amounts of $Os_3(CO)_{10}(CH_3CN)_2$ as catalysts to activate benzimidazole, achieving selective C4–H bond activation (Scheme 4). Among three Os metals, one Os metal (orange one) is proposed to coordinate to benzimidazoles and then direct the other Os metal (purple one) to activate aryl C4–H bond. This is the first example of metal-ligation bonding bimetallic anchoring catalysis for site-selective C–H bond activation.

Then in 1992, the first catalytic version was reported by Moore and co-workers [14], who used $Ru_3(CO)_{12}$ cluster as a catalyst, providing a C2–H acylation of pyridine and derivatives with CO and olefins as acyl source (Scheme 5). The cluster framework was proposed to remain intact during the catalytic cycle because the Ru-pyridine complex cannot generate pyridyl ketone product when it was treated with photolysis, but the mononuclear Ru metal complex can do. In addition, the reaction showed the first-order rate dependence on the concentration of $Ru_3(CO)_{12}$, which also supported cluster catalysis. The presence of extra ligands in the cluster had a strong influence on the reactivity of C–H bond activation. For example, $Ru_3(CO)_{11}(PPh_3)$ was much less active and $Ru_3(CO)_9(PPh_3)_3$ completely shut down the reaction. These results further suggested that the coordination of substrate with the cluster was critical to the reactivity. A possible mechanism was proposed as follows: the coordination of pyridine to the Ru cluster was followed by directed *ortho*-metalation, olefin insertion, migratory carbonyl insertion and reductive elimination, affording acylated pyridines with branched or linear selectivity.

Although Moore's system exhibited high catalytic turnover frequencies and moderate yield, the reaction requires a large excess of pyridine. In 1996, Murai and coworkers [15a] found that a similar catalytic system can be applied to C4−H alkenylation of imidazoles, achieving a range of 4-acyl imidazoles in high yields with imidazoles as limiting reagents (Scheme 6). Later, they found that various other heterocycles were also well compatible with the reaction, providing a series of aryl C−H acylated products in up to 80% yields [15b], which are not easily accessed through traditional catalytic modes.

In 2007, Suzuki and coworkers [16] used ruthenium complexes **Ru-1** and **Ru-2** to investigate C–H activation of pyridines, and obtained a novel bimetal-catalyzed dehydrogenative coupling reaction of pyridines (Scheme 7).

A variety of substituents at C4-position, such as methoxy, methyl, ethoxycarbonyl, and dimethylamino groups, are well tolerated, providing a series of 2,2′-bipyridines in up to 64% yield. Stoichiometric reactions of di-nuclear complexes with pyridine showed that two pyridyl moieties coordinated to the same ruthenium center in *cis* geometry with head-to-head configuration, and the other Ru center activated C–H bonds to form two new C–Ru bonds, indicating a Ru-ligated Ru–Ru

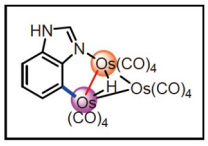

Scheme 4 Os-ligated Os–Os BAC for C–H activation of benzimidazoles (color online).

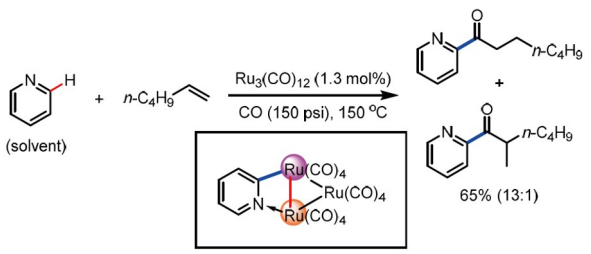

Scheme 5 Ru-ligated Ru–Ru BAC for C2–H acylation of pyridines (color online).

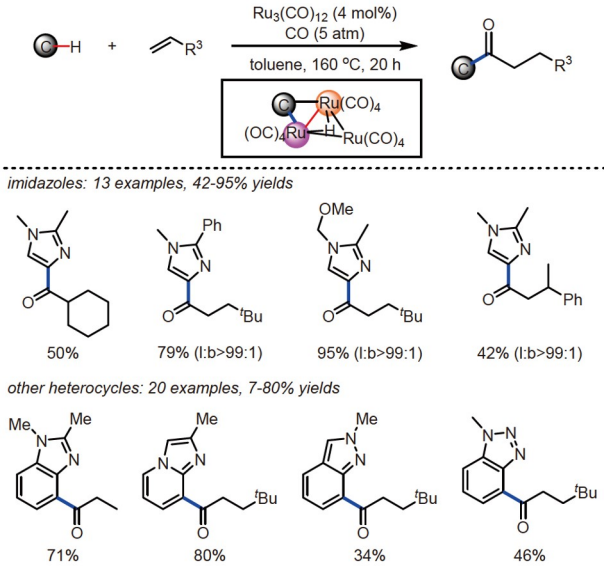

Scheme 6 Ru-ligated Ru–Ru BAC for C–H acylation of imidazoles (color online).

bimetal anchoring catalysis in this reaction.

Except for the above-mentioned metal-ligated bimetallic anchoring catalysis, there is another sole example without metal ligation, in which two metals are proposed to directly ligate each other for C–H activations. In 2011, Chang and co-workers [17] reported a Rh(NHC)-catalyzed C8-selective arylation of quinolines with bromoarenes in the presence of ^{t}BuONa (Scheme 8). They found that the use of a carbene ligand together with $Rh_2(OAc)_4$ as a precatalyst was critical to high C8–H selectivity. Otherwise, C2–H arylation would dominate. Under the optimized conditions, a variety of substituted quinolines and aryl bromides were well tolerated in the reaction. Compared with Bergman-Ellman's Rh-catalyst system that delivered C2-arylation of quinolines with significant base-inhibition effect [18], the current system generates distinctive selectivity and reactivity, suggesting a different mechanism. To explain the result, the authors proposed an Rh–Rh bonding anchoring catalysis (**Int1**). However, a four-membered rhodacycle involving a monomeric Rh-NHC species (**Int2**) still cannot be ruled out.

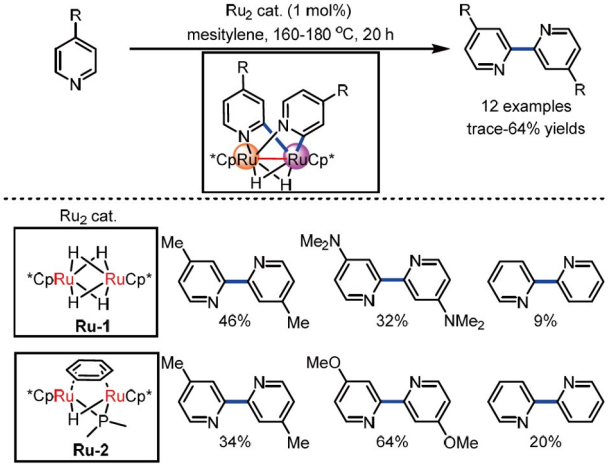

Scheme 7 Ru-ligated Ru–Ru BAC for dehydrogenative coupling of pyridines (color online).

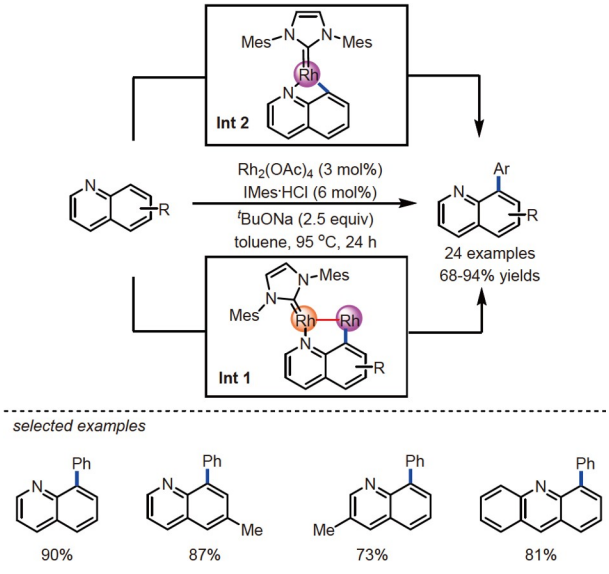

Scheme 8 Rh–Rh BAC without metal ligation for C8-arylation of quinolines (color online).

3 Anion-ligated BAC

Beyond metal clusters that can well accommodate two metals together, metal anions such as hydride, halide and alkyl group also prove to be good linkers to joint two metals.

In 2011, Ogoshi and co-workers [19] reported a Ni-catalyzed intermolecular [3+2] cycloaddition reaction of cyclopropyl ketone and alkynes in the presence of organoaluminum (Scheme 9). They found that the use of Me_2AlCl significantly elevated the reactivity to give a quantitative yield, suggesting that Me_2AlCl was a more optimal Lewis acid than $AlMe_3$. When an isolable six-membered oxa-nickelacycle was treated with alkyne and Me_2AlCl, a π-allylnickel complex bearing a Cl-bridging bond was observed. On the basis of this result, the authors proposed that $AlMe_2Cl$ played dual roles in the reaction: (1) coordination with cyclopropyl ketone, thus reducing C–C bond strength; (2) combination of Al and Ni through a Cl-bridging bond, thus directing Ni for C–C bond activation.

In 2012, Driver's group [20] reported a Ni-catalyzed C7–H selective alkenylation of pyridotriazole with equivalent amounts of $AlMe_3$ (Scheme 10). The order of addition of reagents was crucial to the reaction efficiency: high yields were obtained reproducibly only when triazolopyridine was premixed with $AlMe_3$ before the addition of phosphine and $Ni(cod)_2$. The authors speculated that such an addition order could generate proper coordination of the nickel catalyst with the aluminum *via* a methyl-bridging bond, thus orienting the substrate for selective oxidative addition of C7–H bond.

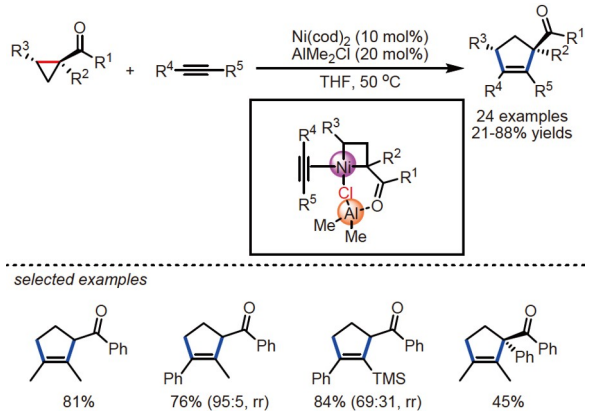

Scheme 9 Cl-ligated Ni–Al BAC for [3+2] cycloaddition (color online).

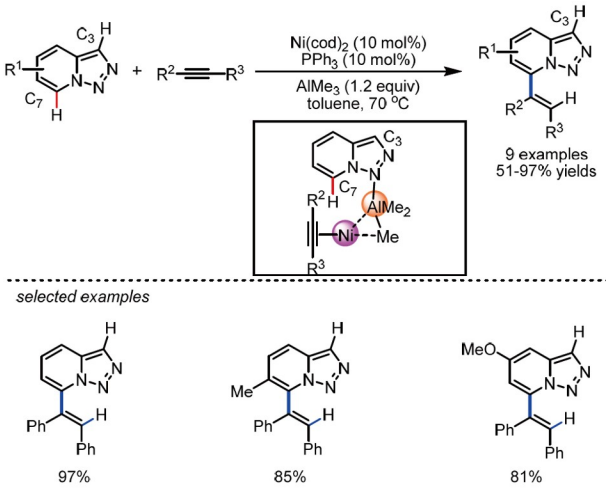

Scheme 10 Me-ligated Ni–Al BAC for C–H alkenylation of triazolopyridines (color online).

4 Ligand-ligated BAC

Although metal ligation and anion ligation can provide good linkages between two metals for synergistic anchoring catalysis, these linkages are still too simplified to provide more versatile functions, for example, long-distance synergism of two metals and stereoselective control. In this context, the use of bifunctional ligand as a linker to ligate two metals simultaneously becomes a new option, because a ligand would not only afford a highly adjustable steric and electronic environment around two metals, but also would allow good enantioselective control by incorporating proper chiral backbone. According to different types of anchoring metals, these reactions can be divided into alkali metal-anchoring type, transition metal-anchoring type and main-group metal-anchoring type.

4.1 Alkali metal as an anchoring metal

In 2017, Chattopadhyay and co-workers [21] reported a *para*-selective borylation of aromatic esters under ligand-ligated K–Ir bimetallic catalysis (Scheme 11).

In this reaction, they designed an L-shaped ligand that contained a bipyridine motif and a 2-quinolone motif. The former coordinated to Ir metal, and the latter generated an alcoholic potassium species that bound the ester group. Finally, the combination of K and Ir bimetallic catalyst successfully furnished a remote C–H bond borylation of arenes *via* synergistic anchoring catalysis.

To confirm the non-covalent (C=O···K–O) interaction between the substrates and the ligand, the authors conducted several control experiments. First, when O atom of the optimal ligand was protected by a methyl group, *para*/*meta* selectivity decreased to 1.9/1 from the original 33/1. Second, in the presence of 10 mol% of 18-crown-6 that would have strong coordination with potassium ion, *para*-selectivity was greatly inhibited. These results indicated that the interaction between the potassium ion and the carbonyl group is crucial to *para*-selectivity.

In 2018, with the same catalytic system, Chattopadhyay's group [22] achieved a *meta*-C–H borylation of aromatic amides (Scheme 12). Similarly, the interaction between the O–K group and an amide group is important in controlling regioselectivity. But the switch of aryl substituent from the ester group to an amide group resulted in reversion of *para* selectivity to *meta* selectivity of arenes, which was probably attributed to a configuration change of macrocyclic transition state.

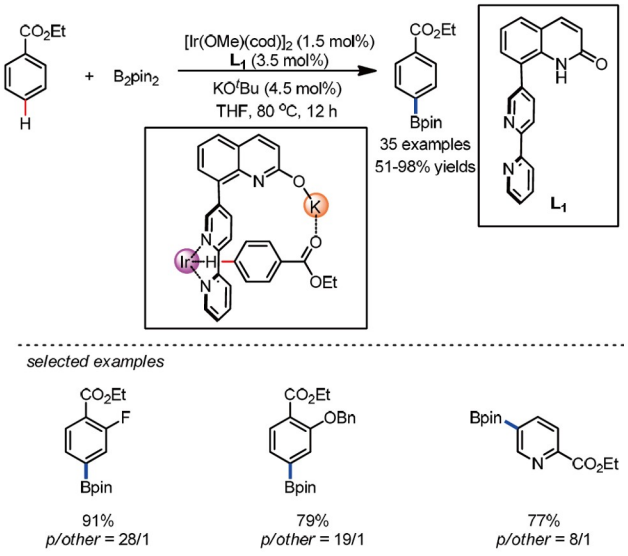

Scheme 11 Ligand-ligated K–Ir BAC for *para*-C–H borylation of aromatic esters (color online).

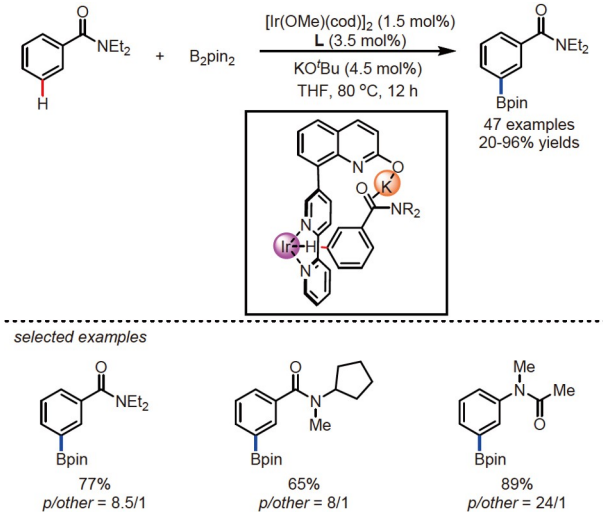

Scheme 12 Ligand-ligated K–Ir BAC for *meta*-C–H borylation of aromatic amides (color online).

4.2 Transition metal as an anchoring metal

4.2.1 Pd–Pd bimetallic catalysis

In 2017, Yu and co-workers [23] reported a new type of bifunctional ligand bearing a bissulfonamide motif and a pyridine motif, with which they realized selective C–H alkenylation of 3-phenylpyridine (Scheme 13). In the reaction, the bissulfonamide motif of the ligand coordinated to one Pd metal to provide an anchoring site for the substrate, and the pyridine motif coordinated to the other Pd metal to activate the remote C–H bond of the aromatic ring.

Following this success, Yu's group continued to explore selective C–H alkenylation of quinolines in the same work (Scheme 14). A new ligand bearing a pyridine-2,6-dicarboxamide motif and a nitrile motif was designed to accommodate quinoline structure. The pyridine motif coordinated to one Pd metal, thus forming a substrate anchoring site, and the nitrile group interacted with the other Pd metal, thus acting as a catalyst to activate C–H bond. Despite one equivalent of ligands required for obtaining a reasonable yield, the reaction provided a highly selective C5–H alkenylation of quinolines in the presence of stoichiometric AgOAc and 10 mol% $Pd(OAc)_2$. This work represents a breakthrough in C–C bond formation *via* bimetallic anchoring catalysis, because all previous ligand-ligated anchoring catalysis are limited to C–H borylation reactions [8–10].

Inspired by this strategy, Maiti's group designed a series of similar bifunctional ligands (Scheme 15), and applied them to develop various types of selective alkenylation or alkylation reactions of quinolones [24], pyridyl-arenes [25] and thiazoles [26] with acrylates or allylic alcohols, achieving good yields and up to excellent site selectivity. These results further demonstrate that bimetallic anchoring catalysis is a powerful strategy for non-directed selective C–H activation.

By combining ligand-ligated bimetallic anchoring catalysis with a transient norbornene mediator strategy, Yu and co-workers [27] developed a selective arylation of benzoazines including quinolines and benzothiazoles, with a reversal selectivity from previous C5 selectivity to C6 selectivity (Scheme 16). This new selectivity is not easily accessible by other methods, demonstrating that the combination of anchoring catalysis and other strategy is a powerful tool for remote C–H bond activation.

4.2.2 Zn–Ir bimetallic catalysis

Recently, Gramage-Doria and co-workers [28] designed a

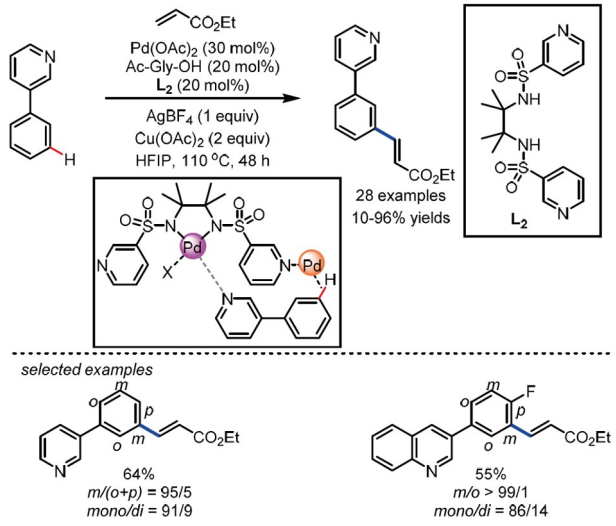

Scheme 13 Ligand-ligated Pd–Pd BAC for *meta*-C–H alkenylation of 3-phenylpyridine (color online).

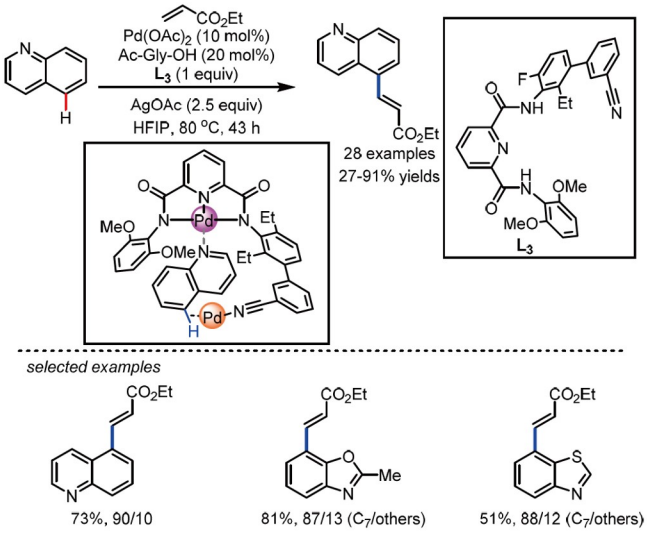

Scheme 14 Ligand-ligated Pd–Pd BAC for C5–H alkenylation of quinolines (color online).

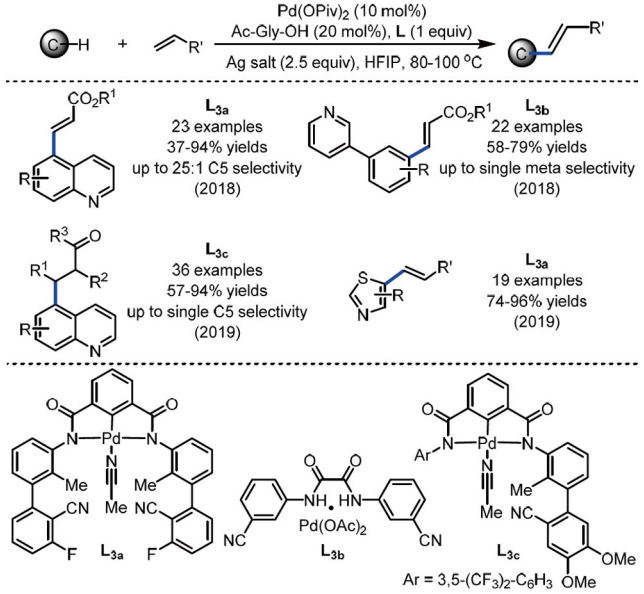

Scheme 15 Ligand-ligated Pd–Pd BAC for C5–H olefination of thiazoles (color online).

porphyrin scaffold bearing a *N*,*N*-bidentate motif (Scheme 17). Porphyrin-Zn acted as an anchoring site to coordinate pyridine derivatives, and then directed bidendate Ir metal to activate C3–H bond of pyridines, providing a range of C3-borylated pyridines and other heterocycles.

4.3 Main-group metal as an anchoring metal

When two transition metals are used in bimetallic anchoring catalysis, a big limitation is the mutual interference of these two metals, because they often have a similar coordinative ability with substrates and ligands. To eliminate potential interference, previous examples in general used two same transition metals such as Pd–Pd in the above-mentioned section. Besides this strategy, another alternative is to use main group metals to act as anchoring metal, because main group metals have the good coordinative ability with substrates and display completely different reactivity from transition metals. With this strategy, mutual interference of two metals would be well inhibited, thus greatly facilitating reaction development.

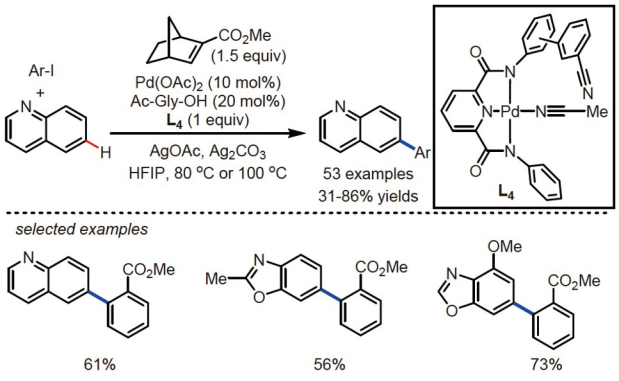

Scheme 16 Bimetallic anchoring catalysis and transient mediator for selective C–H arylation of benzoazines (color online).

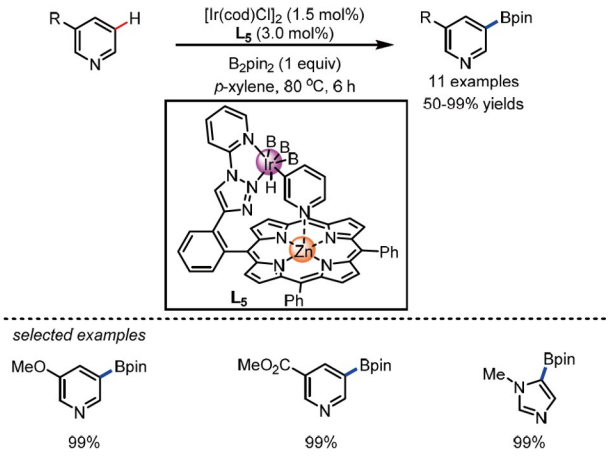

Scheme 17 Ligand-ligated Zn–Ir BAC for C3–H borylation of pyridines (color online).

4.3.1 *Precious metal catalysis*

In 2017, Kuninobu, Kanai and co-workers [29] designed a novel bipyridine ligand containing a boryl group. Taking advantage of the coordination of a sulfur atom in substrates with the boron group, they realized *ortho*-borylation of thioanisole derivatives (Scheme 18). Control experiment with 4,4-di-*tert*-butyl bipyridine (dtbpy) as a ligand gave poor *ortho*-selectivity, and additionally, the electronic property of the boron group also has a strong influence on the reactivity and *ortho*-selectivity. These results suggested a key role of the boryl group of the ligand in the reaction.

Considering that Al-Lewis acids have a stronger Lewis acidity than that of boron reagents, in 2018, Nakao and co-workers [30] designed a phosphine ligand-ligated Rh–Al catalyst for C–H activation of pyridines (Scheme 19). Owing to the fact that aluminum has highly ionic character, which often results in high instability of orgnoaluminum reagents and their difficult preparation, a multi-dentate nitrogen-containing motif was incorporated into the ligand to provide better coordination with aluminum species, thus enhancing the stability of Al species.

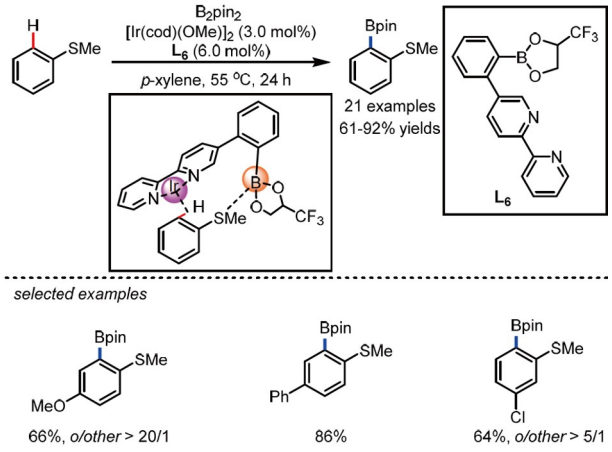

Scheme 18 Ligand-ligated B–Ir BAC for *ortho*-C–H borylation of thioanisoles (color online).

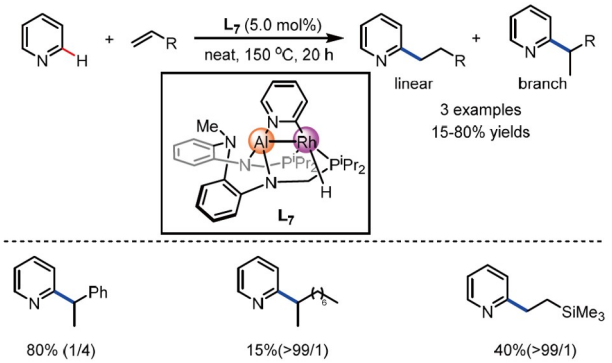

Scheme 19 Ligand-ligated Al–Rh BAC for C2-alkylation of pyridines (color online).

With this ligand, a ligand-ligated Al−Rh complex was synthesized and characterized. Although charge-transfer between two nitrogens and aluminum decreased Lewis acidity of the aluminum center, this catalytic system still worked well, smoothly furnishing a C2-alkylation of pyridines with alkenes.

In addition, they found that a similar catalyst can also effectively facilitate a C2–H silylation of pyridines, providing a series of silylated heterocyles in up to 94% yield (Scheme 20) [31].

To achieve C–H functionalization at C3 positions of pyridines, in 2019, Nakao and co-workers [32] developed a 1,10-phenanthroline-based bifunctional ligand bearing an alkylborane moiety (Scheme 21). Through the coordination of the boron group with pyridine, Ir catalyst was directed to activate C3–H bond of pyridines. This work is the first example of high C3-selective borylation of pyridines, solving a long-term challenge in the field of C–H borylation of pyridines.

The same report also examined selective C–H borylation of arenes bearing an amide carboxylate. However, the above-mentioned boron-containing ligand was not so effective because of more electron-rich aromatic C–H bonds. Therefore, they designed a new bifunctional 2,2′-bipyridine ligand bearing an alkylaluminum biphenoxide moiety with stronger Lewis acidity (Scheme 22). With this ligand, Ir catalyst was easily directed to activate *meta*-C−H bond of aromatic rings, providing a *meta*-selective C−H borylation of benzamides. This method showed good tolerance toward a range of functional groups including Lewis basic groups without loss of site-selectivity.

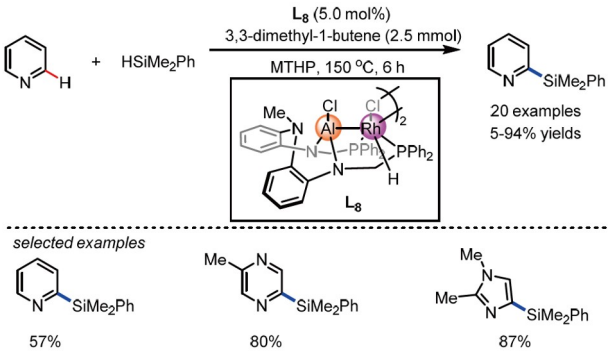

Scheme 20 Ligand-ligated Al–Rh BAC for C2–H silylation of pyridines (color online).

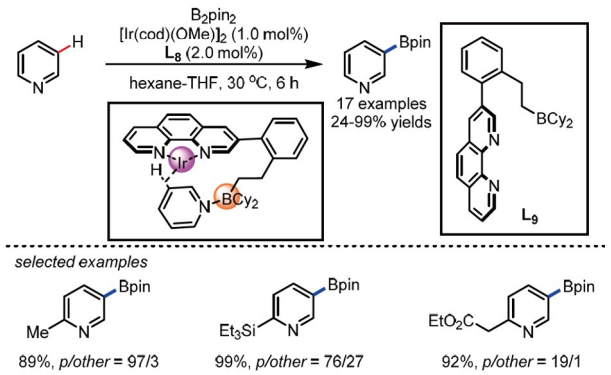

Scheme 21 Ligand-ligated Al–Ir BAC for C3−H borylation of pyridines (color online).

4.3.2 *3d-Transition metal catalysis*

3d-Transition metals are recognized as ideal surrogates of precious metals in organic reactions, because of their high abundance, low price, low bio-toxicity and unique properties [33], while 3d-metal-catalyzed C−H or C−C bond activation has been a challenging task. Relying on bidentate directing groups or pre-activated substrates, C−H or C−C bonds can be smoothly activated by 3d-metals [34]. In contrast, non-directed C−H or C−C bond activation is more difficult to be achieved. Coordination-bonding bimetallic anchoring catalysis has been applied to address this challenge.

On the basis of the seminal racemic work by Nakao and co-workers [35], in 2013, Cramer's group [36] found that chiral phosphine oxide (PO) ligand can promote Ni−Al co-catalyzed C−H cyclizaiton of formamides with alkenes, providing a series of chiral γ-lactams derivatives were constructed with up to 98% yield and up to 95% ee (Scheme 23).

In consideration of superior reactivity and enantioselectivity of this phosphine oxide ligand than that of traditional chiral phosphines, the authors proposed that phosphine oxide may tautomerize into a trivalent phosphinous acid isomer, which would act as a bifunctional ligand to bind both nickel and aluminum, thus providing coordination-bonding anchoring catalysis in the reaction. The detailed mechanism is depicted as below (Scheme 24): phosphinic acid reacts with $AlMe_3$ to generate adduct **A**, which binds Ni(0) to form an active catalyst **B**. After the coordination of aluminum with formamide (**C**), nickel is directed to activate formyl C–H

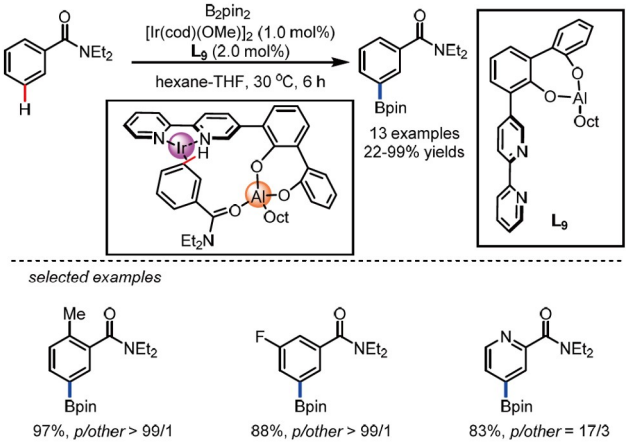

Scheme 22 Ligand-ligated Al–Ir BAC for *meta*-C−H borylation of benzamides (color online).

bond. Subsequent alkene insertion and reductive elimination results in final γ-lactams.

To confirm such a hypothesis, the authors prepared a putative intermediate **PO$_1$**-Al through the reaction of **PO$_1$** ligand with Me_2AlCl (Scheme 25), and found that the use of 0.25 mol% of the complex can ensure high reactivity without additional $AlMe_3$ and PPh_3. This discovery on phosphine oxide ligand-binding Ni and Al for C−H bond activation is an important breakthrough, providing the first bimetallic anchoring catalysis of 3d-metals.

In 2017, Ye's group [37] investigated a [3+2] cycloaddition reaction of cyclopropyl carboxamides with alkynes, which has been an elusive challenge for a long time. Ogoshi and co-workers [19] have reported the cycloaddition of cyclopropyl ketones and alkynes, in which Cl-ligated Ni–Al bimetal was proposed to be an active catalyst. However, this catalyst was ineffective to cyclopropyl carboxamides that cannot form stable oxa-nickelacycle intermediates from the originally generated 4-membered nickelacycle in the reaction. To stabilize such an instable nickelacycle, Ye's group proposed to use a bifunctional ligand instead of a weak Cl bridge to ligate Ni and Al for achieving a more stable bicyclic intermediate to promote the reaction. Systematical investigation of ligands revealed that phosphine oxides were an optimal ligand that can well ligate Ni and Al to smoothly furnish a [3+2] cycloaddition reaction of cyclopropyl carboxamides with alkynes, providing a wide range of 5-membered products in up to 97% yield.

After the completion of the racemic reaction, an enantioselective reaction was then realized by using a naphthyl-substituted chiral tartrate-derived PO (**PO$_2$**) as an optimal ligand together with additional tertiary phosphine (Scheme 26) [37], providing a series of synthetically useful cyclopentenyl carboxamides in up to 99% yield and 94% ee. This example further demonstrated that phosphine oxide-ligated Ni–Al bimetallic system could be a powerful anchoring catalytic system for a broad range of reactions.

A plausible mechanism was proposed in Scheme 27: phosphine oxide reacts with $AlMe_3$ and $Ni(cod)_2$ to generate *in-situ* bimetallic catalyst **D**, which coordinates to a substrate and then direct Ni for C−C bond activation. Subsequent alkyne insertion and reductive elimination provided the corresponding alkenylated product and regenerated the active catalyst **D**. The *in-situ* formed PO−Ni−Al combination probably played a triple role: activating cyclopropane substrate, directing nickel to undergo oxidative addition and stabilizing the *in situ* formed nickelacycle. NMR studies

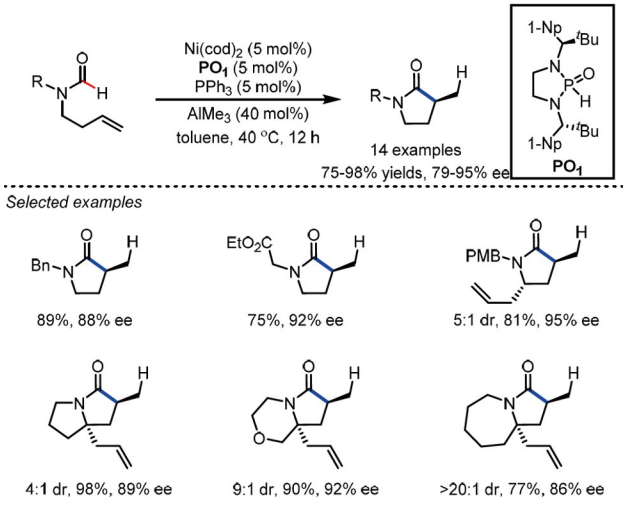

Scheme 23 PO-ligated Ni−Al BAC for C–H cyclization of formamides with alkenes (color online).

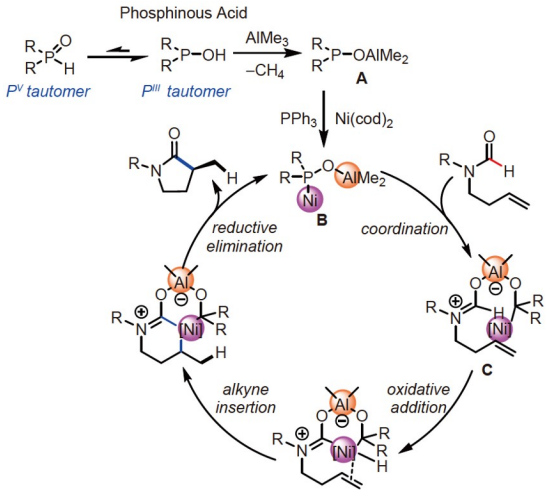

Scheme 24 Proposed mechanism (color online).

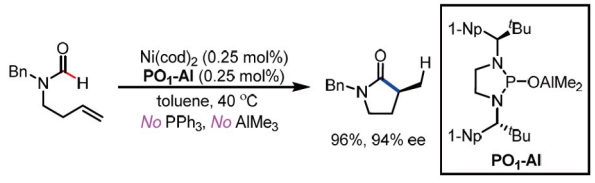

Scheme 25 Reactivity of phosphine oxide-Al complex (color online).

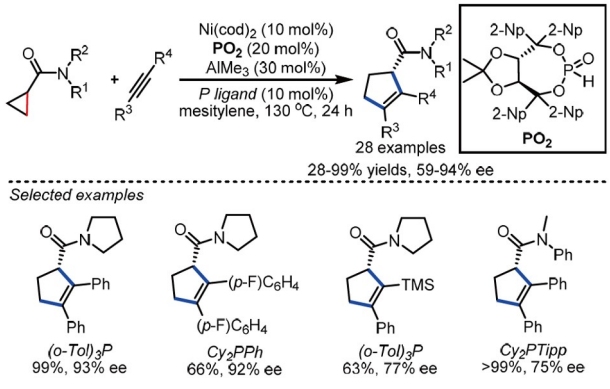

Scheme 26 PO-ligated Ni−Al BAC for enantioselective cycloaddition of cyclopropyl carboxamides with alkynes (color online).

were conducted to confirm this mechanism. Both ^{1}H and ^{31}P NMR spectra showed that $Ph_2P(O)H$ and $AlMe_3$ easily transformed into P−O−Al complex, which then coordinated to nickel to form a Ni−P−O−Al bimetallic catalyst. With 10 mol% of this catalyst, the model reaction gave the desired product in 54% yield.

On the basis of this work, Ye's group [38] further extended this phosphine oxide-ligated bimetallic anchoring catalysis to other inert bond activation reactions. In 2018, C–H cyclization of benzimidazoles with alkenes was achieved by using Taddol-derived phosphine oxide (**PO_3**)-ligated Ni–Al bimetallic anchoring catalysis, providing a series of bi- and polycyclic imidazoles with β-stereocenter in up to 98% yield and up to >99% ee (Scheme 28). Owing to high reactivity and selectivity, even vulnerable C−Br bond still survived in this reaction. In contrast, the previous Rh-catalyzed version in general required high loadings of Rh (10–20 mol%) and harsh conditions (160–180 °C), rendering enantioselective control quite difficult.

A similar catalytic cycle as depicted in Scheme 29: bimetallic catalyst **E** is formed first and then coordinates to benzoimidazole. Subsequently, Ni was directed to activate C−H bond *via* either ligand-to-ligand H transfer or oxidative addition pathway. The following alkene insertion and reductive elimination delivers the product and regenerates the active catalytic species for the next catalytic cycle. In mechanistic experiments, the authors synthesized imidazole-$AlMe_3$ and imidazole-$AlMe_3$-$Ph_2P(O)H$ complexes, and characterized them with ^{1}H and ^{31}P NMR spectra. Upon treatment with stoichiometric nickel, the imidazole-$AlMe_3$-$Ph_2P(O)H$ can afford the desired product in nearly quantitative yield.

Nakao and co-workers [39] reported Ni−Al co-catalyzed cyclization of double C−H bonds of formamides with alkynes. However, due to the need of activating two C−H bonds, the reaction is very challenging, and only sterically-demanding alkyl formamides are compatible. In 2020, Ye's group [40] found that the use of bulky diamino phosphine oxide (**PO_4**) to ligate Ni and Al can significantly enhance the reactivity, and a broad range arylformamides were compatible with the reaction for the first time, providing a series of pyridone compounds in up to 97% yield (Scheme 30). Control experiments showed that commonly-used ligands

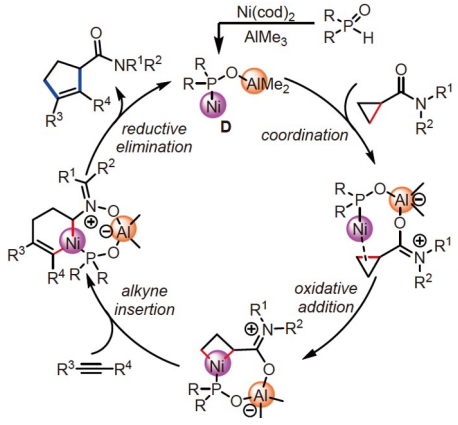

Scheme 27 Proposed mechanism (color online).

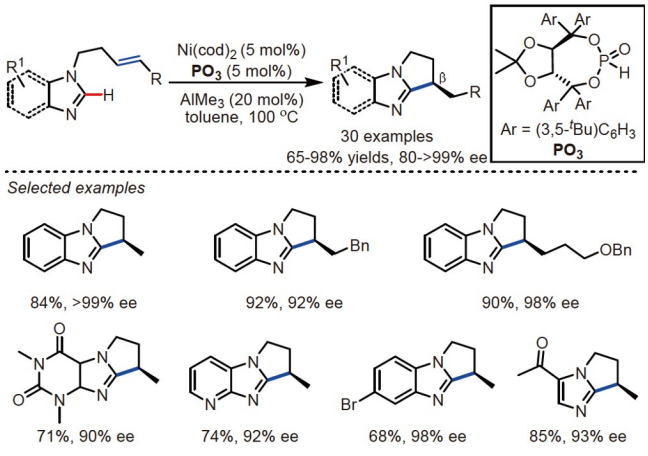

Scheme 28 PO-ligated Ni−Al BAC for enantioselective C−H cyclization of imidazoles with alkenes (color online).

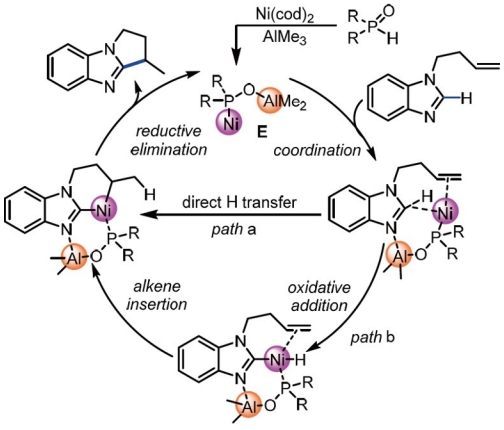

Scheme 29 Proposed mechanism (color online).

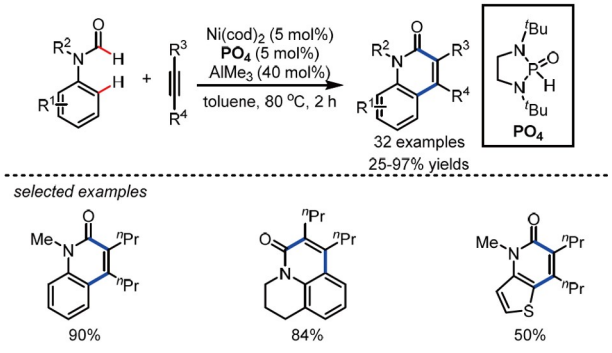

Scheme 30 PO-ligated Ni−Al BAC for non-directed dual C−H annulation of arylformamides with alkynes (color online).

such as monophosphines, bisphosphines, and *N*-herteocyclic carbenes were all ineffective, often resulting in hydrocarbamoylation products *via* direct reductive elimination after the first formyl C−H bond activation.

A possible reaction mechanism was proposed in Scheme 31: *in-situ* formed catalytic species PO−Ni−Al coordinates to formamide, and then Ni is directed to activate the first formyl C–H bond of the formyl group *via* oxidative addition. Subsequent alkyne insertion and the second aryl C–H bond activation, followed by the second alkyne insertion and reductive elimination, generate the final product. This example confirmed that ligand-ligated bimetal anchoring catalysis could promote catalytic reactivity more than traditional metal catalysis and even bimetallic catalysis without a ligand linker.

Following this racemic reaction, Ye's group [41] then designed a BINOL-derived chiral PO ligand (**PO_6**) and developed an enantioselective twofold C–H annulation of ferrocene-based formamides and alkynes. Various diaryl alkynes and dialkyl alkynes were well tolerated, providing a series of chiral ferrocenes in 40%−98% yield and 93%−99% ee (Scheme 32). This is the first example of enantioselective non-directed twofold C−H annulation, demonstrating that bimetallic anchoring catalysis could provide an efficient tool for enantioselective control of inert bond activation.

Recently, the dual C−H annulation reaction model was extended to *N*-aryl imidazole by Ye's group [42] (Scheme 33). A range of N-aryl imidazoles was catalyzed to react with alkynes, providing a series of polycyclic aza-quinolines in 48%−95% yields.

Beyond enantioselective control, PO-ligated Ni−Al bimetallic anchoring catalysis also proves effective to site selectivity control. Direct C–H functionalization of enamides is of great importance for obtaining diverse amide derivatives [43]. However, most of the previous reactions are limited to the functionalization of vinylic β-C(sp^2)−H bonds, while the activation of unreactive β′-C(sp^3)−H bonds is quite challenging and has been scarcely explored. A sole example was reported by Glorius and co-workers [44] by installing an ester group as a directing group into substrates to enable an Rh-catalyzed cyclization. Despite an efficient method, the requirement of an ester directing group greatly restricts the scope of substrates and the complexity of products. With the use of taddol-derived phosphine oxide (**PO_6**) ligand-ligated Ni−Al bimetallic catalyst, Ye's group [45] recently achieved selective β′-C(sp^3)−H cleavage of *N*-formamide enamides, providing a series of 2-pyridones in 58%−99% yields (Scheme 34). Various cyclic or acyclic enamides and alkynes were well compatible with the reaction. DFT calculation showed that bimetallic catalyst reacts with the substrate to form a rigid cyclic intermediate, which benefits the activation of more flexible C(sp^3)−H bond.

Selective C–H functionalization of 2-pyridones has been

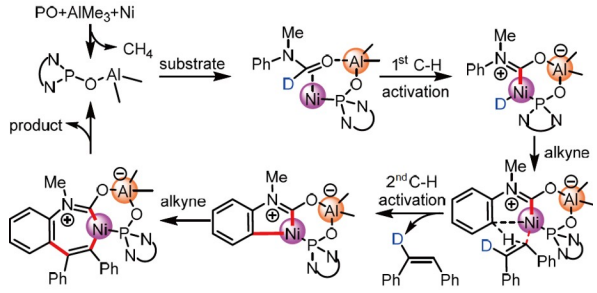

Scheme 31 Proposed mechanism (color online).

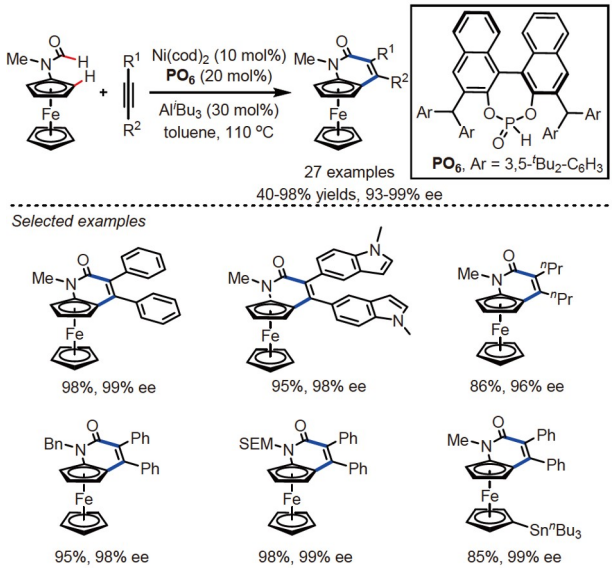

Scheme 32 PO-ligated Ni−Al BAC for enantioselective twofold C–H annulation of ferrocene-based formamides (color online).

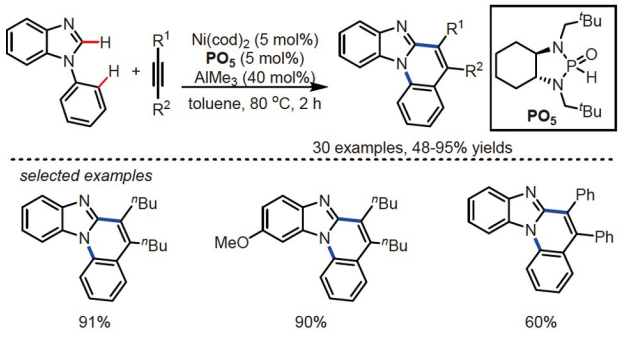

Scheme 33 PO-ligated Ni−Al BAC for dual C−H annulation of *N*-aryl imidazole with alkynes (color online).

an important research topic because of their wide existence in bioactive compounds. Traditional high-valent transition metal-enabled electrophilic activation is prone to activating more electron-rich C5–H bond [46], and low-valent transition metal-enabled oxidative activation prefers to activating more electron-deficient C6–H bond [47]. In contrast, selective activation of C3–H or C4–H bonds is more difficult.

In 2012, Li and co-workers [48] incorporated a methyl

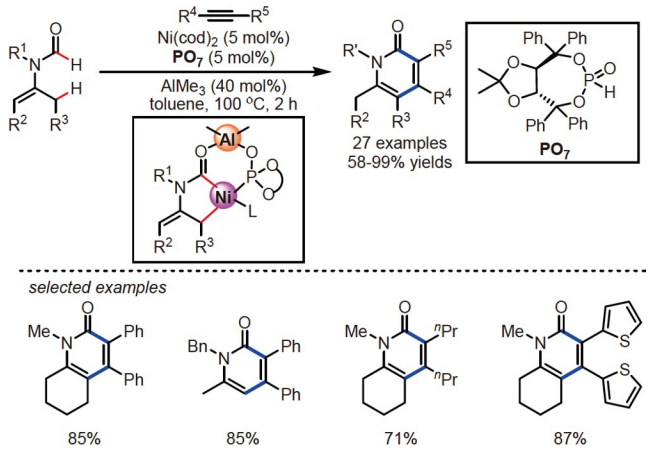

Scheme 34 PO-ligated Ni−Al BAC for selective C(sp^3)−H cleavage of enamides (color online).

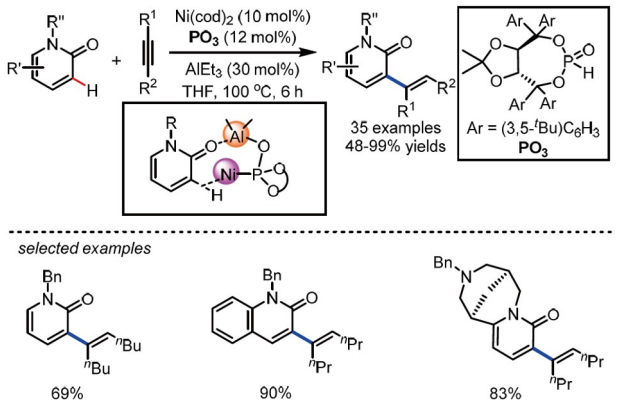

Scheme 35 PO-ligated Ni−Al BAC for C3−H alkenylation of 2-pyridones (color online).

group at C4 position to achieve a C3–H alkenylation of 2-pyridiones. Despite an important advance, such substrate modification leads to a narrow range of substrates. Recently Ye's group [49] found that the use of PO-ligated Ni–Al bimetallic catalyst can selectively activate C3–H bond of 2-pyridone without substrate modification, providing various C3-alkenylated 2-pyridones in up to 99% yields (Scheme 35). In the reaction, the pre-coordination of the substrate with the bimetallic catalyst provided an important directing effect, which resulted in preferential activation of C3–H bond other than C6–H bond or C4–H bond. Mechanistic experiments and DFT calculations confirmed the critical role of PO–Ni–Al catalyst in reversing conventional C6/C4-selectivity to C3-selectivity.

This success on selective C–H functionalization of 2-pyridones has spurred another exploration on C3–H alkenylation of pyridines because of their resembling structures. Although Yu's group [50] used a Pd(II) catalyst to achieve a C3-selective alkenylation in 2011, the reactivity was quite low, in general requiring for a large excess of pyridine (at least 16 equivalents) with high concentration (at least 8 M) for reasonable yields. This requirement rendered complex pyridines incompatible with the reaction. In 2008, Nakao and co-workers [51] proved that the use of Ni–Al co-catalyst can significantly enhance the reactivity of pyridine C–H activation, but the alkenylation was restricted to electron-deficient C2/C4 positions, other than the desired C3 position.

Recently, Ye's group [52] used ligand-ligated Ni–Al anchoring catalysis to achieve a breakthrough in addressing this challenge. A new bifunctional carbene ligand was designed to ligate both Ni and Al, thus forming a long-distance bimetallic backbone to allow remote C3–H activation of pyridines (Scheme 36). Under the optimized conditions, a series of C3-alkenylated pyridines were obtained in 43%–99% yields with up to 98:2 C3 selectivity. More importantly, various complex pyridines can be alkenylated smoothly at

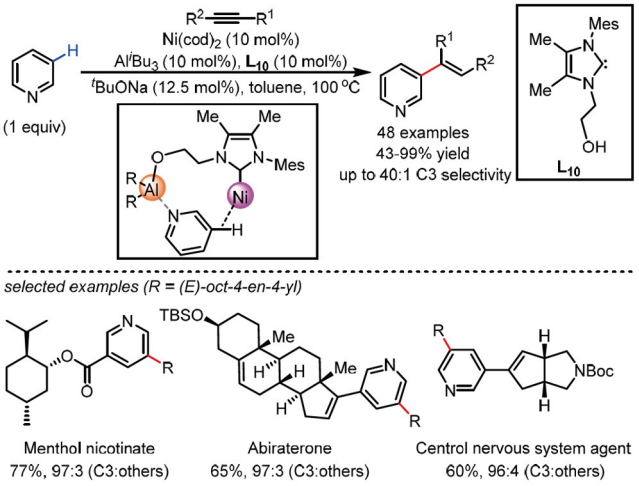

Scheme 36 Selective C3-alkenylation of pyridine (color online).

C3-position of pyridine motif using one equivalent of substrates. Control experiments showed that the carbene ligand had a strong influence on both the reactivity and the selectivity control.

To further extend the application of bimetallic anchoring catalysis in remote control, Ye's group recently investigated C–CN bond activation reaction. The development of C–CN bond activation is of great importance and has received wide attention. Big progress has been achieved by using Ni and Al co-catalysis by Nakao and coworkers [53], while the enantioselective version has been a formidable challenge, because traditional chiral bidentate ligands would significantly inhibit the reactivity because of saturated coordination of nickel. Only limited success on enantioselective intramolecular reactions has been achieved [54], but enantioselective intermolecular versions remain an elusive challenge.

In 2020, Ye's group [55] first tried to use phosphine oxide-ligated Ni–Al catalyst to explore an intermolecular annula-

tion reaction, but the linear structure of nitriles cannot be accommodated onto PO–Ni–Al bimetallic framework, rendering the reaction ineffective. In this context, they used a diol-binding bis-aluminum to form a macrocyclic framework, which easily accommodated the linear nitrile and furnished a highly enantioselective intermolecular C–CN bond activation reaction (Scheme 37). With racemic phosphine as a ligand and chiral diol as a linker between two Al metals, the reaction smoothly preceeded under mild reaction conditions, providing various indenes bearing chiral all-carbon quaternary centers in 32%–91% yields and 73%–98% ee. DFT calculations suggested that an irreversible alkyne insertion was an enantioselectivity-determining step, and the weak interaction of the aryl group of the phosphine ligand with Al species was critical to the reactivity and the selectivity.

5 Conclusions and outlook

Although directing group strategy has been widely applied to a large variety of transition metal-catalyzed C–H or C–C bond activation reactions, its inherent limitations, including the need for special directing groups and extra synthetic steps for installation and removal of such directing groups, call for the development of new strategies. Anchoring catalysis, which resembles the enzyme's catalytic mode, has stood out as a promising strategy for non-directed C–H or C–C bond activation. In this strategy, reversible anchoring interaction is a key character that differentiates anchoring catalysis from traditional directing-group strategy. Reversible anchoring interactions proved feasible in C–H or C–C bond activation including reversible covalent bonding, H-bonding, coordinative bonding, and ion-pair bonding. Among them, coordinative bonding can exhibit superior catalytic reactivity than others, because coordinative bonding not only affords good coordination of catalysts with substrates, but also it displays good compatibility with substrates and reaction conditions. By virtue of these advantages, bimetallic coordinative-bonding anchoring catalysis has received increasing attention in recent years.

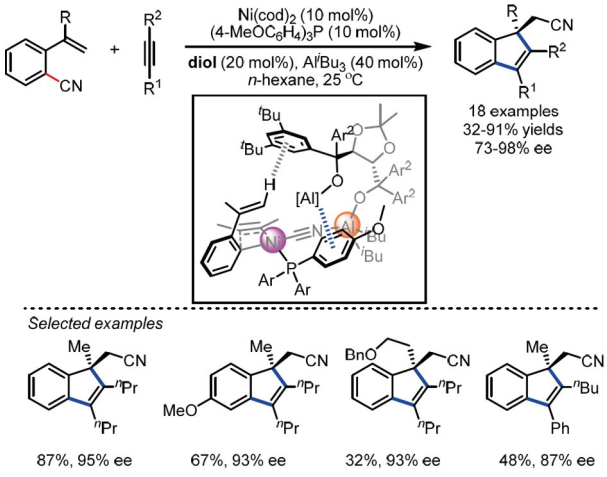

Scheme 37 Macrocyclic Ni–Al BAC for enantioselective C–CN bond activation (color online).

The earliest bimetallic anchoring catalysis can be traced back to direct metal-ligated mode in metal clusters. But successful examples are scarce, and limited metal combination renders site- and stereo-selective control difficult. The second-generation bimetallic anchoring catalysis is to use metal anion to ligate two metals, especially two different metals. Despite expanding the scope of metal combinations, the types of these bimetallic catalysts are still rare because of the narrow range of metal anions available. When a proper bifunctional ligand is used to ligate two metals, the latest-generation bimetallic anchoring catalysis emerges. This method allows versatile modification of bimetallic catalysts, including the tuning of the steric environment around metals, electronic property of metal centers and even the distance between two metals. However, a great difficulty for this catalytic mode lies in accurate identification between two metals and two anchoring sites of the ligand. Otherwise, mutual interference between them would significantly inhibit the reaction. That is why only limited ligand types such as phosphine oxides, bipyridines, biphosphine and carbenes, and limited reaction types have been developed up to now.

However, impressive results such as unique reactivity, site selectivity and high enantioselectivity achieved in various challenging reactions demonstrate that the ligand-ligated bimetallic anchoring catalysis is one of the most efficient tools for a wide range of inert chemical bond transformations. In the near future, more types of novel ligands and reactions will be developed.

Acknowledgements This work was supported by the National Natural Science Foundation of China (91856104, 21871145), the Tianjin Applied Basic Research Project and Cutting-Edge Technology Research Plan (19JCZDJC37900) and "Frontiers Science Center for New Organic Matter", Nankai University (63181206).

Conflict of interest The authors declare no conflict of interest.

1 (a) Kakiuchi F, Chatani N. *Adv Synthesis Catal*, 2003, 345: 1077–1101; (b) Godula K, Sames D. *Science*, 2006, 312: 67–72; (c) Yamaguchi J, Yamaguchi AD, Itami K. *Angew Chem Int Ed*, 2012, 51: 8960–9009

2 For selected reviews on C−H activation:(a) Dyker G. *Angew Chem Int Ed*, 1999, 38: 1698–1712; (b) Ritleng V, Sirlin C, Pfeffer M. *Chem Rev*, 2002, 102: 1731–1770; (c) Kakiuchi F, Murai S. *Acc Chem Res*, 2002, 35: 826–834; (d) Seregin IV, Gevorgyan V. *Chem Soc Rev*, 2007, 36: 1173–1193; (e) Lewis JC, Bergman RG, Ellman JA. *Acc Chem Res*, 2008, 41: 1013–1025; (f) Giri R, Shi BF, Engle KM, Maugel N, Yu JQ. *Chem Soc Rev*, 2009, 38: 3242–3272; (g) Colby DA, Bergman RG, Ellman JA. *Chem Rev*, 2010, 110: 624–655; (h) Wencel-Delord J, Dröge T, Liu F, Glorius F. *Chem Soc Rev*, 2011, 40: 4740–4761; (i) Yang L, Huang H. *Chem Rev*, 2015, 115: 3468–3517;

(j) Tao P, Jia Y. *Sci China Chem*, 2016, 59: 1109–1125; (k) Newton CG, Wang SG, Oliveira CC, Cramer N. *Chem Rev*, 2017, 117: 8908–8976; (l) Diesel J, Cramer N. *ACS Catal*, 2019, 9: 9164–9177; For selected reviews on C−C activation: (m) Jun CH. *Chem Soc Rev*, 2004, 33: 610–618; (n) Murakami M, Matsuda T. *Chem Commun*, 2011, 47: 1100–1105; (o) Chen F, Wang T, Jiao N. *Chem Rev*, 2014, 114: 8613–8661; (p) Dermenci A, Coe JW, Dong G. *Org Chem Front*, 2014, 1: 567–581; (q) Marek I, Masarwa A, Delaye PO, Leibeling M. *Angew Chem Int Ed*, 2015, 54: 414–429; (r) Souillart L, Cramer N. *Chem Rev*, 2015, 115: 9410–9464; (s) Chen PH, Billett BA, Tsukamoto T, Dong G. *ACS Catal*, 2017, 7: 1340–1360; (t) Murakami M, Ishida N. *Chem Rev*, 2021, 121: 264–299

3 For selected examples on intramolecular C–H activation, see: (a) Ames DE, Opalko A. *Tetrahedron*, 1984, 40: 1919–1925; (b) Echavarren AM. J Am Chem Soc. 2006, 128: 1066−1067; (c) Basolo L, Beccalli EM, Borsini E, Broggini G. *Tetrahedron*, 2009, 65: 3486–3491

4 For selected reviews on directing group, see: (a) Jun CH, Moon CW, Lee DY. *Chem Eur J*, 2002, 8: 2422–2428; (b) Wang J, Chen W, Zuo S, Liu L, Zhang X, Wang J. *Angew Chem Int Ed*, 2012, 51: 12334–12338; (c) Corbet M, De Campo F. *Angew Chem Int Ed*, 2013, 52: 9896–9898; (d) Rouquet G, Chatani N. *Angew Chem Int Ed*, 2013, 52: 11726–11743; (e) Zhang M, Zhang Y, Jie X, Zhao H, Li G, Su W. *Org Chem Front*, 2014, 1: 843–895; (f) Chen Z, Wang B, Zhang J, Yu W, Liu Z, Zhang Y. *Org Chem Front*, 2015, 2: 1107–1295; (g) Castro LCM, Chatani N. *Chem Lett*, 2015, 44: 410–421; (h) Wang K, Hu F, Zhang Y, Wang J. *Sci China Chem*, 2015, 58: 1252–1265; (i) Zhu RY, Farmer ME, Chen YQ, Yu JQ. *Angew Chem Int Ed*, 2016, 55: 10578–10599; (j) Zhang L, Fang DC. *Org Chem Front*, 2017, 4: 1250–1260; (k) Rej S, Ano Y, Chatani N. *Chem Rev*, 2020, 120: 1788–1887; (l) Ali W, Prakash G, Maiti D. *Chem Sci*, 2021, 12: 2735–2759; (m) Dutta U, Maiti S, Bhattacharya T, Maiti D. *Science*, 2021, 372: eabd5992; (n) Suseelan AS, Dutta A, Lahiri GK, Maiti D. *Trends Chem*, 2021, 3: 188–203; (o) Dey A, Sinha SK, Achar TK, Maiti D. *Angew Chem Int Ed*, 2019, 58: 10820–10843

5 For selected reviews see: (a) Wu Y, Shi B. *Chin J Org Chem*, 2020, 40: 3517–3535; (b) Liao G, Zhang T, Lin ZK, Shi BF. *Angew Chem Int Ed*, 2020, 59: 19773–19786; (c) Becica J, Dobereiner GE. *Org Biomol Chem*, 2019, 17: 2055–2069; (d) Omann L, Königs CDF, Klare HFT, Oestreich M. *Acc Chem Res*, 2017, 50: 1258–1269; (e) Davis HJ, Phipps RJ. *Chem Sci*, 2017, 8: 864–877; (f) Chen DF, Han ZY, Zhou XL, Gong LZ. *Acc Chem Res*, 2014, 47: 2365–2377; (g) Dong XQ, Zhao Q, Li P, Chen C, Zhang X. *Org Chem Front*, 2015, 2: 1425–1431; (h) Dydio P, Reek JNH. *Chem Sci*, 2014, 5: 2135–2145; (i) Raynal M, Ballester P, Vidal-Ferran A, van Leeuwen PWNM. *Chem Soc Rev*, 2014, 43: 1660–1733; (j) Tan KL. *ACS Catal*, 2011, 1: 877–886; (k) Rousseau G, Breit B. *Angew Chem Int Ed*, 2011, 50: 2450–2494; (l) Sawamura M, Ito Y. *Chem Rev*, 1992, 92: 857–871

6 For selected reviews on non-covalent interaction, see: (a) Haldar C, Hoque M E, Bisht R, Chattopadhyay B. *Tetrahedron Lett*, 2018, 59: 1269–1277; (b) Rasheed OK, Sun B. *ChemistrySelect*, 2018, 3: 5689–5708; (c) Mahmudov KT, Gurbanov AV, Guseinov FI, Guedes da Silva MFC. *Coord Chem Rev*, 2019, 387: 32–46; (d) Kuninobu Y, Torigoe T. *Org Biomol Chem*, 2020, 18: 4126–4134; (e) Pandit S, Maiti S, Maiti D. *Org Chem Front*, 2021, https://doi.org/10.1039/d1qo00452b; (f) Trouvé J, Gramage-Doria R. *Chem Soc Rev*, 2021, 50: 3565–3584

7 For selected reviews on reversible covalent bonding, see: (a) Sun H, Guimond N, Huang Y. *Org Biomol Chem*, 2016, 14: 8389–8397; (b) Afewerki S, Córdova A. *Chem Rev*, 2016, 116: 13512–13570; (c) Zhao Q, Poisson T, Pannecoucke X, Besset T. *Synthesis*, 2017, 49: 4808–4826; (d) Kim DS, Park WJ, Jun CH. *Chem Rev*, 2017, 117: 8977–9015; (e) Gandeepan P, Ackermann L. *Chem*, 2018, 4: 199–222; (f) Bhattacharya T, Pimparkar S, Maiti D. *RSC Adv*, 2018, 8: 19456–19464; (g) St John-Campbell S, Bull JA. *Org Biomol Chem*, 2018, 16: 4582–4595; (h) Niu B, Yang K, Lawrence B, Ge H. *ChemSusChem*, 2019, 12: 2955–2969

8 For selected examples on H-bonding, see: (a) Kuninobu Y, Ida H, Nishi M, Kanai M. *Nat Chem*, 2015, 7: 712–717; (b) Lu X, Yoshigoe Y, Ida H, Nishi M, Kanai M, Kuninobu Y. *ACS Catal*, 2019, 9: 1705–1709; (c) Bai ST, Bheeter CB, Reek JNH. *Angew Chem Int Ed*, 2019, 58: 13039–13043; (d) Reyes RL, Sato M, Iwai T, Suzuki K, Maeda S, Sawamura M. *Science*, 2020, 369: 970–974; (e) Genov GR, Douthwaite JL, Lahdenperä ASK, Gibson DC, Phipps RJ. *Science*, 2020, 367: 1246–1251

9 For selected examples on ion-pair bonding, see: (a) Davis HJ, Mihai MT, Phipps RJ. *J Am Chem Soc*, 2016, 138: 12759–12762; (b) Davis HJ, Genov GR, Phipps RJ. *Angew Chem Int Ed*, 2017, 56: 13351–13355; (c) Mihai MT, Davis HJ, Genov GR, Phipps RJ. *ACS Catal*, 2018, 8: 3764–3769; (d) Lee B, Mihai MT, Stojalnikova V, Phipps RJ. *J Org Chem*, 2019, 84: 13124–13134; (e) Montero Bastidas JR, Oleskey TJ, Miller SL, Smith Iii MR, Maleczka Jr. RE. *J Am Chem Soc*, 2019, 141: 15483–15487

10 For selected examples on electrostatic interactions, see: (a) Chattopadhyay B, Dannatt JE, Andujar-De Sanctis IL, Gore KA, Maleczka Jr. RE, Singleton DA, Smith III MR. *J Am Chem Soc*, 2017, 139: 7864–7871; (b) Chaturvedi J, Haldar C, Bisht R, Pandey G, Chattopadhyay B. *J Am Chem Soc*, 2021, 143: 7604–7611

11 For selected reviews on bimetallic catalysis with both two metals as catalysts, see: (a) van den Beuken EK, Feringa BL. *Tetrahedron*, 1998, 54: 12985–13011; (b) Rowlands GJ. *Tetrahedron*, 2001, 57: 1865–1882; (c) Matsunaga S, Shibasaki M. *Bull Chem Soc Jpn*, 2008, 81: 60–75; (d) Pérez-Temprano MH, Casares JA, Espinet P. *Chem Eur J*, 2012, 18: 1864–1884; (e) Park J, Hong S. *Chem Soc Rev*, 2012, 41: 6931–6943; (f) Hetterscheid DGH, Chikkali SH, de Bruin B, Reek JNH. *ChemCatChem*, 2013, 5: 2785–2793; (g) Mankad NP. *Chem Eur J*, 2016, 22: 5822–5829; (h) Fu J, Huo X, Li B, Zhang W. *Org Biomol Chem*, 2017, 15: 9747–9759; (i) Pye DR, Mankad NP. *Chem Sci*, 2017, 8: 1705–1718

12 For selected reviews on bimetallic catalysis without directing effect, see: (a) Wang YX, Ye M. *Sci China Chem*, 2018, 61: 1004–1013; (b) Hu Y, Wang C. *Acta Physico-Chim Sin*, 2019, 35: 913–922

13 Shapley JR, Samkoff DE, Bueno C, Churchill MR. *Inorg Chem*, 1982, 21: 634–639

14 Moore EJ, Pretzer WR, O'Connell TJ, Harris J, LaBounty L, Chou L, Grimmer SS. *J Am Chem Soc*, 1992, 114: 5888–5890

15 (a) Chatani N, Fukuyama T, Kakiuchi F, Murai S. *J Am Chem Soc*, 1996, 118: 493–494; (b) Fukuyama T, Chatani N, Tatsumi J, Kakiuchi F, Murai S. *J Am Chem Soc*, 1998, 120: 11522–11523

16 Kawashima T, Takao T, Suzuki H. *J Am Chem Soc*, 2007, 129: 11006–11007

17 Kwak J, Kim M, Chang S. *J Am Chem Soc*, 2011, 133: 3780–3783

18 (a) Berman AM, Lewis JC, Bergman RG, Ellman JA. *J Am Chem Soc*, 2008, 130: 14926–14927; (b) Berman AM, Bergman RG, Ellman JA. *J Org Chem*, 2010, 75: 7863–7868

19 Tamaki T, Ohashi M, Ogoshi S. *Angew Chem Int Ed*, 2011, 50: 12067–12070

20 Liu S, Sawicki J, Driver TG. *Org Lett*, 2012, 14: 3744–3747

21 Hoque ME, Bisht R, Haldar C, Chattopadhyay B. *J Am Chem Soc*, 2017, 139: 7745–7748

22 Bisht R, Hoque ME, Chattopadhyay B. *Angew Chem Int Ed*, 2018, 57: 15762–15766

23 Zhang Z, Tanaka K, Yu JQ. *Nature*, 2017, 543: 538–542

24 Ramakrishna K, Biswas JP, Jana S, Achar TK, Porey S, Maiti D. *Angew Chem Int Ed*, 2019, 58: 13808–13812

25 Achar TK, Ramakrishna K, Pal T, Porey S, Dolui P, Biswas JP, Maiti D. *Chem Eur J*, 2018, 24: 17906–17910

26 Achar TK, Biswas JP, Porey S, Pal T, Ramakrishna K, Maiti S, Maiti D. *J Org Chem*, 2019, 84: 8315–8321

27 Shi H, Lu Y, Weng J, Bay KL, Chen X, Tanaka K, Verma P, Houk KN, Yu JQ. *Nat Chem*, 2020, 12: 399–404

28 Trouvé J, Zardi P, Al-Shehimy, S, Roisnel T, Gramage-Doria R. *Angew Chem Int Ed*, 2021, 60: 18006–18013

29 Li HL, Kuninobu Y, Kanai M. *Angew Chem Int Ed*, 2017, 56: 1495–

1499
30 Hara N, Saito T, Semba K, Kuriakose N, Zheng H, Sakaki S, Nakao Y. *J Am Chem Soc*, 2018, 140: 7070–7073
31 Hara N, Uemura N, Nakao Y. *Chem Commun*, 2021, 57: 5957–5960
32 Yang L, Uemura N, Nakao Y. *J Am Chem Soc*, 2019, 141: 7972–7979
33 For selected reviews on first-row transition metal-catalysis, see: (a) Su B, Cao ZC, Shi ZJ. *Acc Chem Res*, 2015, 48: 886–896; (b) Zweig JE, Kim DE, Newhouse TR. *Chem Rev*, 2017, 117: 11680–11752; (c) Chen J, Guo J, Lu Z. *Chin J Chem*, 2018, 36: 1075–1109; (d) Obligacion JV, Chirik PJ. *Nat Rev Chem*, 2018, 2: 15–34; (e) Peng JB, Wu FP, Wu XF. *Chem Rev*, 2019, 119: 2090–2127; (f) Alig L, Fritz M, Schneider S. *Chem Rev*, 2019, 119: 2681–2751; (g) Wang R, Luan Y, Ye M. *Chin J Chem*, 2019, 37: 720–743
34 For recent reviews on 3d-metals catalyzed C–H functionalization, see: (a) Khake SM, Chatani N. *Chem*, 2020, 6: 1056–1081; (b) Yamaguchi J, Muto K, Itami K. *Top Curr Chem (Z)*, 2016, 374: 55; (c)Cai XH, Xie B. ARKIVOC, 2015, 184–211; (d) Gandeepan P, Müller T, Zell D, Cera G, Warratz S, Ackermann L. *Chem Rev*, 2019, 119: 2192–2452; (e) Loup J, Dhawa U, Pesciaioli F, Wencel-Delord J, Ackermann L. *Angew Chem Int Ed*, 2019, 58: 12803–12818; (f) Woźniak Ł, Cramer N. *Trends Chem*, 2019, 1: 471–484; (g) Liu Y, Xia Y, Shi B. *Chin J Chem*, 2020, 38: 635–662; (h) Khake SM, Chatani N. *Trends Chem*, 2019, 1: 524–539; (i) Chu JCK, Rovis T. *Angew Chem Int Ed*, 2018, 57: 62–101; (j) Feng YN, Shi BF. Chin J Org Chem, 2021, https://doi.org/10.6023/cjoc202104004
35 (a) Nakao Y, Idei H, Kanyiva KS, Hiyama T. *J Am Chem Soc*, 2009, 131: 5070–5071; (b) Miyazaki Y, Yamada Y, Nakao Y, Hiyama T. *Chem Lett*, 2012, 41: 298–300
36 Donets PA, Cramer N. *J Am Chem Soc*, 2013, 135: 11772–11775
37 Liu QS, Wang DY, Yang ZJ, Luan YX, Yang JF, Li JF, Pu YG, Ye M. *J Am Chem Soc*, 2017, 139: 18150–18153
38 Wang YX, Qi SL, Luan YX, Han XW, Wang S, Chen H, Ye M. *J Am Chem Soc*, 2018, 140: 5360–5364
39 Nakao Y, Morita E, Idei H, Hiyama T. *J Am Chem Soc*, 2011, 133: 3264–3267
40 Wang YX, Zhang FP, Luan YX, Ye M. *Org Lett*, 2020, 22: 2230–2234
41 Chen H, Wang YX, Luan YX, Ye MC. *Angew Chem Int Ed*, 2020, 132: 9528–9532
42 Qi SL, Li Y, Li JF, Zhang T, Luan YX, Ye M. *Org Lett*, 2021, 23: 4034–4039
43 (a) Gigant N, Chausset-Boissarie L, Gillaizeau I. *Chem Eur J*, 2014, 20: 7548–7564; (b) Zhu T, Xie S, Rojsitthisak P, Wu J. *Org Biomol Chem*, 2020, 18: 1504–1521
44 Rakshit S, Patureau FW, Glorius F. *J Am Chem Soc*, 2010, 132: 9585–9587
45 Wang RH, Li JF, Li Y, Qi SL, Zhang T, Luan YX, Ye M. *ACS Catal*, 2021, 11: 858–864
46 For selected examples on C5−H functionalization *via* electrophilic activation pathway, see: (a) Itahara T, Ouseto F. *Synthesis*, 1984, 1984: 488–489; (b) Li Y, Xie F, Li X. *J Org Chem*, 2016, 81: 715–722; (c) Maity S, Das D, Sarkar S, Samanta R. *Org Lett*, 2018, 20: 5167–5171
47 For selected examples on selective C6−H functionalization *via* oxidative addition pathway, see: (a) Tamura R, Yamada Y, Nakao Y, Hiyama T. *Angew Chem Int Ed*, 2012, 51: 5679–5682; (b) Nakao Y, Idei H, Kanyiva KS, Hiyama T. *J Am Chem Soc*, 2009, 131: 15996–15997
48 Chen Y, Wang F, Jia A, Li X. *Chem Sci*, 2012, 3: 3231–3236
49 Yin G, Li Y, Wang RH, Li JF, Xu XT, Luan YX, Ye M. *ACS Catal*, 2021, 11: 4606–4612
50 Ye M, Gao GL, Yu JQ. *J Am Chem Soc*, 2011, 133: 6964–6967
51 (a) Nakao Y, Kanyiva KS, Hiyama T. *J Am Chem Soc*, 2008, 130: 2448–2449; For relevant examples, see: (b) Tsai CC, Shih WC, Fang CH, Li CY, Ong TG, Yap GPA. *J Am Chem Soc*, 2010, 132: 11887–11889; (c) Nakao Y, Yamada Y, Kashihara N, Hiyama T. *J Am Chem Soc*, 2010, 132: 13666–13668; (d) Lee WC, Chen CH, Liu CY, Yu MS, Lin YH, Ong TG. *Chem Commun*, 2015, 51: 17104–17107
52 Zhang T, Luan YX, Lam N, Li JF, Li Y, Ye MC, Yu JQ. https://doi.org/10.26434/chemrxiv.13250420.vl
53 (a) Nakao Y, Yada A, Ebata S, Hiyama T. *J Am Chem Soc*, 2007, 129: 2428–2429; (b) Nakao Y, Ebata S, Yada A, Hiyama T, Ikawa M, Ogoshi S. *J Am Chem Soc*, 2008, 130: 12874–12875; (c) Hirata Y, Yukawa T, Kashihara N, Nakao Y, Hiyama T. *J Am Chem Soc*, 2009, 131: 10964–10973; (d) Yada A, Yukawa T, Nakao Y, Hiyama T. *Chem Commun*, 2009, 107: 3931–3933; (e) Nakao Y, Yada A, Hiyama T. *J Am Chem Soc*, 2010, 132: 10024–10026; (f) Yada A, Ebata S, Idei H, Zhang D, Nakao Y, Hiyama T. *BCSJ*, 2010, 83: 1170–1184; (g) Yamada Y, Ebata S, Hiyama T, Nakao Y. *Tetrahedron*, 2015, 71: 4413–4417; (h) Nakai K, Kurahashi T, Matsubara S. *J Am Chem Soc*, 2011, 133: 11066–11068; (i) Nakai K, Kurahashi T, Matsubara S. *Org Lett*, 2013, 15: 856–859; (j) Nakai K, Kurahashi T, Matsubara S. *Tetrahedron*, 2015, 71: 4512–4517
54 (a) Yasui Y, Kamisaki H, Takemoto Y. *Org Lett*, 2008, 10: 3303–3306; (b) Yasui Y, Kinugawa T, Takemoto Y. *Chem Commun*, 2009, 1: 4275–4277; (c) Yasui Y, Kamisaki H, Ishida T, Takemoto Y. *Tetrahedron*, 2010, 66: 1980–1989; (d) Frost GB, Serratore NA, Ogilvie JM, Douglas CJ. *J Org Chem*, 2017, 82: 3721–3726; (e) Dreis AM, Otte SC, Eastwood MS, Alonzi ER, Brethorst JT, Douglas CJ. *Eur J Org Chem*, 2017, 2017(1): 45–48; (f)Hsieh JC, Ebata S, Nakao Y, Hiyama T. *Synlett*, 2010, 1709; (g) Watson MP, Jacobsen EN. *J Am Chem Soc*, 2008, 130: 12594–12595
55 Zhang T, Luan YX, Zheng SJ, Peng Q, Ye M. *Angew Chem Int Ed*, 2020, 59: 7439–7443